

## Supporting Information

### Ultrafine Rh nanoparticles decorated MoSe<sub>2</sub> nanoflowers for efficient alkaline hydrogen evolution reaction

Yuanmeng Zhao<sup>a</sup>, Chenlu Yang<sup>a</sup>, Guixiang Mao<sup>a</sup>, Jun Su<sup>b</sup>, Gongzhen Cheng<sup>a</sup> and Wei Luo<sup>a\*</sup>

<sup>a</sup>College of Chemistry and Molecular Sciences, Wuhan University, Wuhan, Hubei, 430072, P.R. China, Tel.: +86-27-68752366.

\*Corresponding author. E-mail addresses: [wluo@whu.edu.cn](mailto:wluo@whu.edu.cn)

<sup>b</sup>Wuhan National Laboratory for Optoelectronics, Huazhong University of Science and Technology, Wuhan, Hubei, 430074, P.R. China

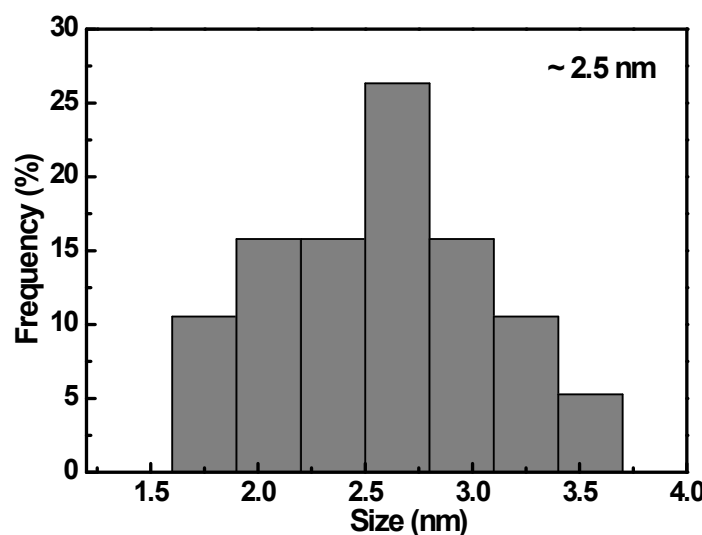


Fig. S1 The size distribution histogram of 8.2 wt% Rh-MoSe<sub>2</sub>.

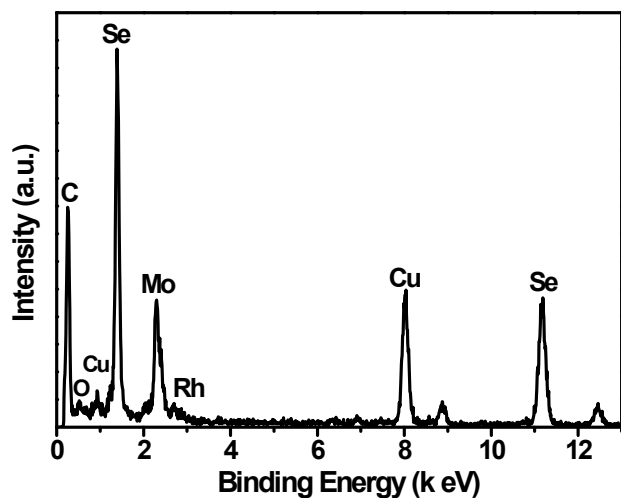


Fig. S2 The EDX spectrum of 8.2 wt% Rh-MoSe<sub>2</sub>.

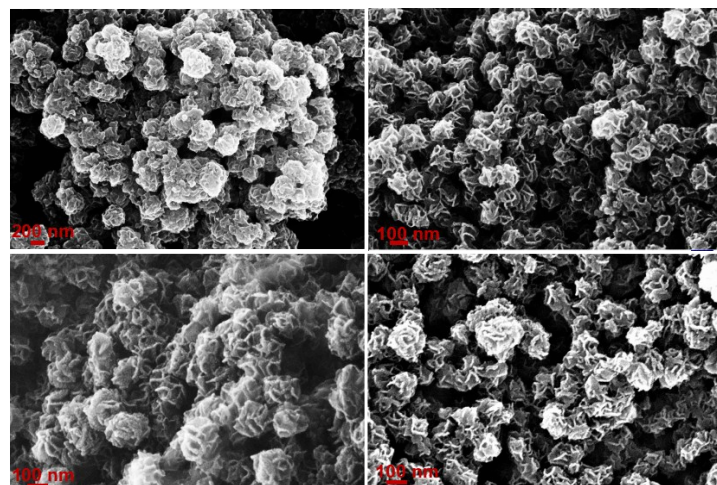


Fig. S3 SEM images of Rh-MoSe<sub>2</sub> with different contents of Rh: (a) pure MoSe<sub>2</sub>; (b) 2.9 wt%; (c) 8.2 wt% and (d) 12.6 wt% of Rh.

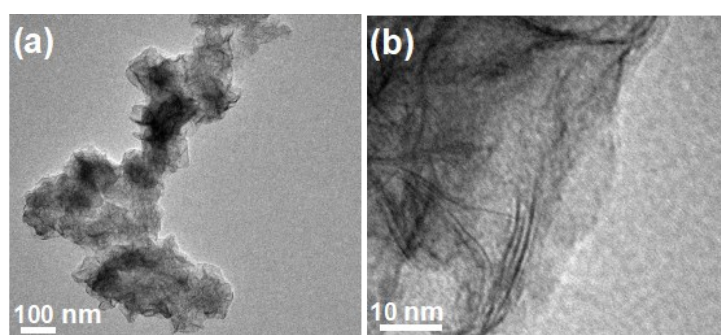


Fig. S4 TEM image of as-synthesized pure MoSe<sub>2</sub>.

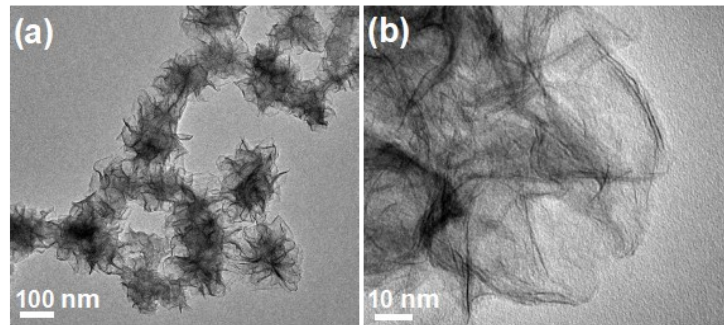


Fig. S5 TEM image of as-synthesized 2.9 wt% Rh-MoSe<sub>2</sub>.

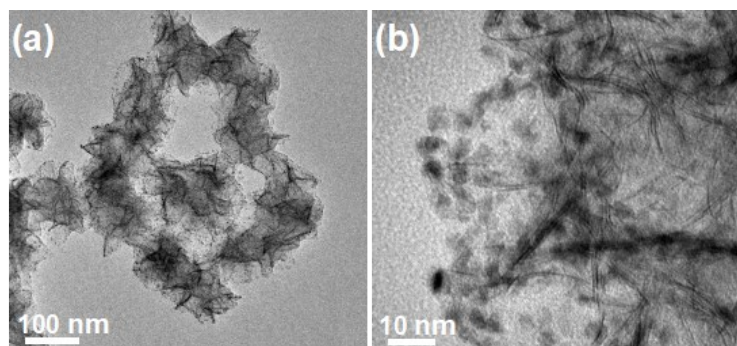


Fig. S6 TEM image of as-synthesized 12.6 wt% Rh-MoSe<sub>2</sub>.

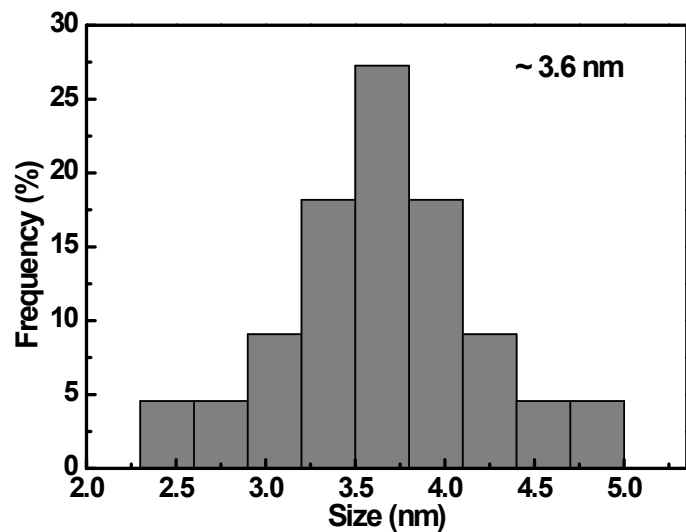


Fig. S7 The size distribution histogram of 12.6 wt% Rh-MoSe<sub>2</sub>.

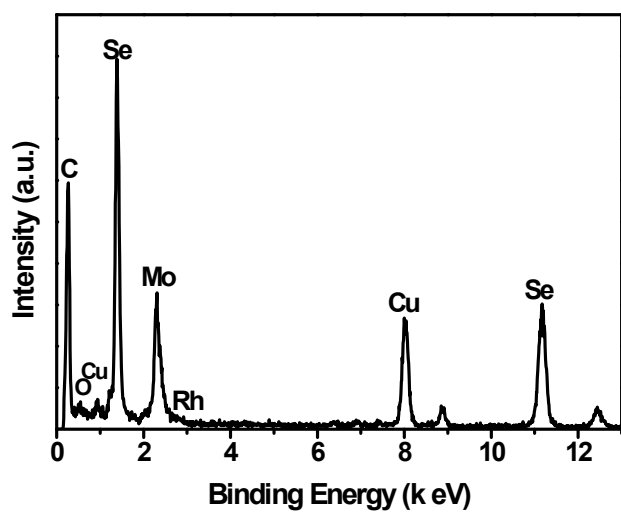


Fig. S8 The EDX spectrum of 2.9 wt% Rh-MoSe<sub>2</sub>.

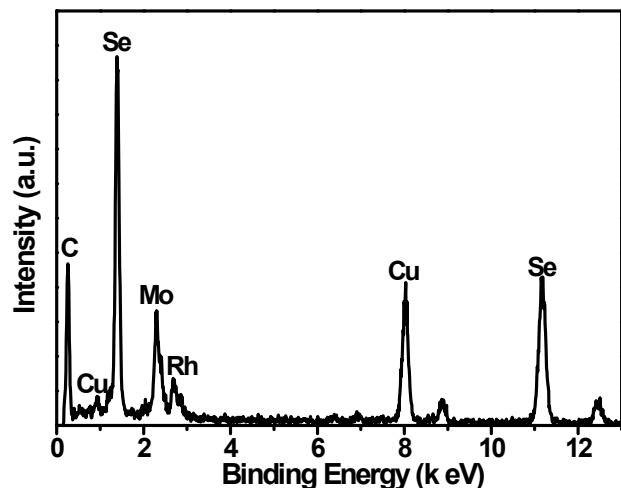


Fig. S9 The EDX spectrum of 12.6 wt% Rh-MoSe<sub>2</sub>.

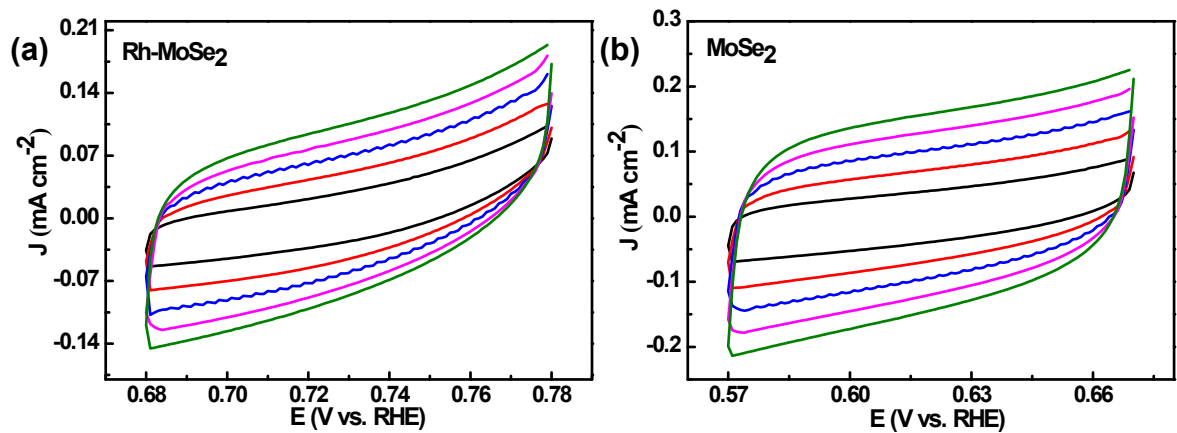


Fig. S10 Electrochemical double layer capacitance curves on wt% Rh-MoSe<sub>2</sub> (a) and MoSe<sub>2</sub> (b) with different scan rates from 50 mV s<sup>-1</sup> to 10 mV s<sup>-1</sup> in 1.0 M KOH.

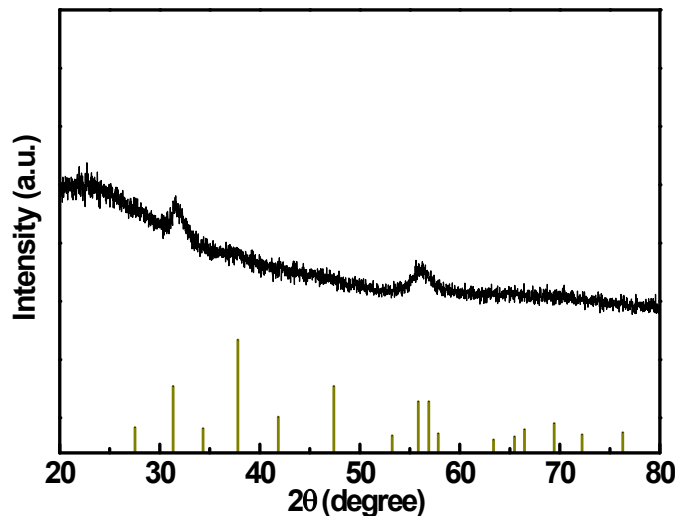


Fig. S11 XRD patterns of the 8.2 wt% Rh-MoSe<sub>2</sub> nanoflowers after chronopotentiometry test.

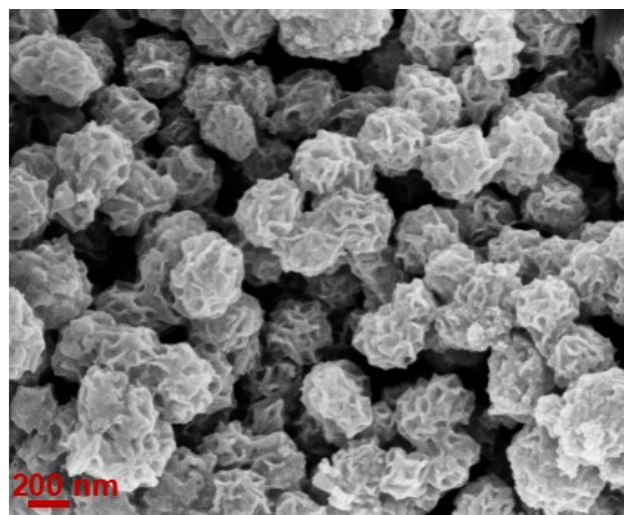


Fig. S12 SEM image of the 8.2 wt% Rh-MoSe<sub>2</sub> nanoflowers after chronopotentiometry test.

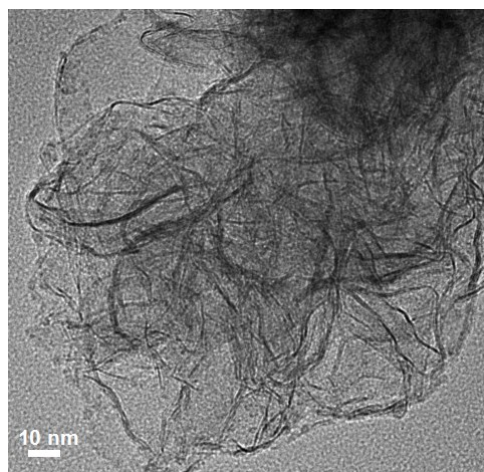


Fig. S13 TEM image of 8.2 wt% Rh-MoSe<sub>2</sub> nanoflowers after stability testing.

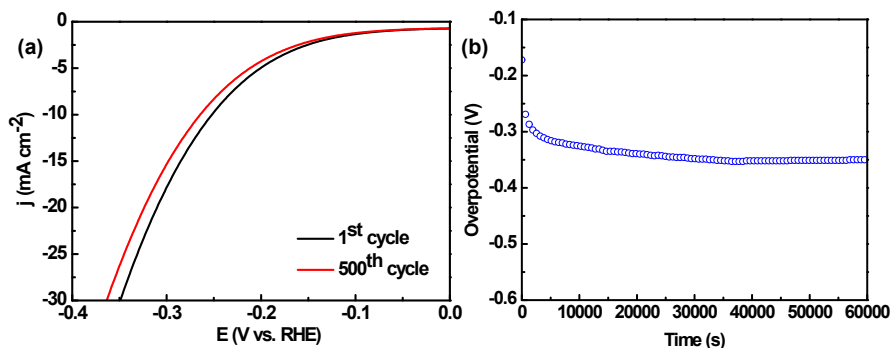


Fig. S14 (a)Polarization curves of MoSe<sub>2</sub> before and after 500 CV cycles. (b) Chronopotentiometric measurements of the HER at 10  $\text{mA cm}^{-2}$  using MoSe<sub>2</sub> as a catalyst.

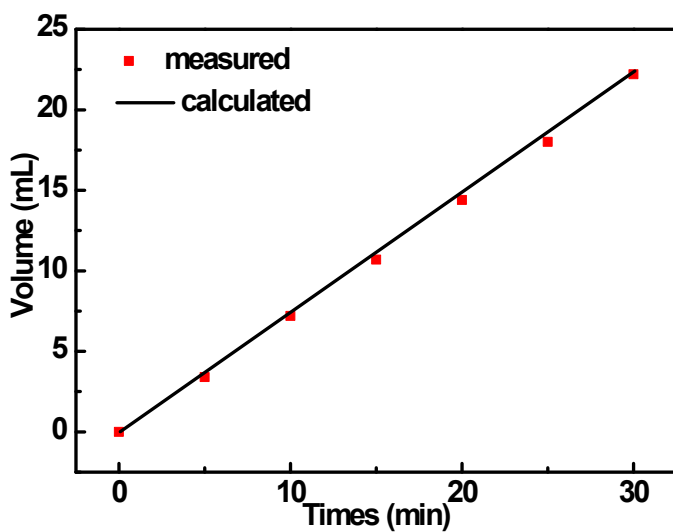


Fig. S13. The amount of hydrogen theoretically calculated and experimentally measured versus time for 8.2 wt% Rh-MoSe<sub>2</sub> in 1.0 M KOH.

Table S1. The raw material of Rh(acac)<sub>3</sub> and the corresponding contents of Rh in Rh-MoSe<sub>2</sub> nanoflowers.

Raw material Rh(acac) <sub>3</sub> (mg)	Rh content in Rh-MoSe <sub>2</sub>	
	Rh (wt%)	
4	2.9	
12	8.2	
20	12.6	

Table S2. Comparison of representative TMDs-based catalysts in 1.0 M KOH.

Catalyst	Substrate	Loading (mg cm <sup>-2</sup> )	$\eta_{10}/(\text{mV})$	Reference
Rh-MoSe <sub>2</sub>	GCE	0.3	73	This work
CoSe <sub>2</sub> /MoSe <sub>2</sub>	GCE	0.204	218	1
CS-MS/rGO-C	GCE	0.57	215	2
MS-CS NTs	GCE	0.57	237	3
Co-WSe <sub>2</sub> /MWNT	GCE	0.25	241	4
2D-MoS <sub>2</sub> /Co(OH) <sub>2</sub>	GCE	~0.285	128	5
Co <sub>9</sub> S <sub>8</sub> @MoS <sub>2</sub>	GCE	~0.4	145	6
MoS <sub>2</sub> /NiS	nickel foam	4.9	92	7
MoWSe alloys	GCE	1	262	8
Ni(OH) <sub>2</sub> /MoS <sub>2</sub>	Carbon cloth	~4.8	80	9

<u>MoSe<sub>2</sub>@Ni<sub>0.85</sub>Se</u>	nickel foam	6.48	117	10
CoS/MoS <sub>2</sub>	GCE	0.18	214	11
Co <sub>3</sub> S <sub>4</sub> /MoS <sub>2</sub> /Ni <sub>2</sub> P NTs	GCE	0.18	178	11
Ru/MoS <sub>2</sub>	Carbon paper	1.0	13	12
MoS <sub>2</sub>  NiS MoO <sub>3</sub>	Ti sheet	2	91	13
MoS <sub>2</sub> -Ni <sub>3</sub> S <sub>2</sub> HNRs/NF	Nickel foam	13	98	14
MoS <sub>2</sub> /Ni <sub>3</sub> S <sub>2</sub>	Nickel foam	9.7	110	15
Ni-MoS <sub>2</sub>	Carbon cloth	0.89	98	16
MoS <sub>2</sub> @Ni/CC	Carbon cloth	4.0	91	17
HF-MoSP	GCE	0.35	119	18
<u>Co<sub>9</sub>S<sub>8</sub>@MoS<sub>2</sub>/CNFs</u>	GCE	0.212	190	19

## References

- [1] G. Zhao, P. Li, K. Rui, Y. Chen, S. X. Dou and W. Sun, *Chem. Eur. J.*, 2018, **24**, 11158.
- [2] B. Wang, Z. Wang, X. Wang, B. Zheng, W. Zhang and Y. Chen, *J. Mater. Chem. A*, 2018, **6**, 12701.
- [3] X. Wang, B. Zheng, B. Yu, B. Wang, W. Hou, W. Zhang and Y. Chen, *J. Mater. Chem. A*, 2018, **6**, 7842.
- [4] G. Zhang, X. Zheng, Q. Xu, J. Zhang, W. Liu and J. Chen, *J. Mater. Chem. A*, 2018, **6**, 4793.
- [5] Z. Zhu, H. Yin, C. -T. He, M. Al-Mamun, P. Liu, L. Jiang, Y. Zhao, Y. Wang, H. -G. Yang, Z. Tang, D. Wang, X. -M. Chen and H. Zhao, *Adv. Mater.*, 2018, **30**, 1801171.

- [6] J. Bai, T. Meng, D. Guo, S. Wang, B. Mao and M. Cao, *ACS Appl. Mater. Interfaces*, 2018, **10**, 1678.
- [7] Z. Zhai, C. Li, L. Zhang, H. -C. Wu, L. Zhang, N. Tang, W. Wang and J. Gong, *J. Mater. Chem. A*, 2018, **6**, 9833.
- [8] O. E. Meiron, V. Kuraganti, I. Hod, R. Bar-Ziv and M. Bar-Sadan, *Nanoscale*, 2017, **9**, 13998.
- [9] B. Zhang, J. Liu, J. Wang, Y. Ruan, X. Ji, K. Xu, C. Chen, H. Wan, L. Miao and J. Jiang, *Nano Energy*, 2017, **37**, 74.
- [10] C. Wang, P. Zhang, J. Lei, W. Dong and J. Wang, *Electrochim. Acta*, 2017, **246**, 712.
- [11] H. Lin, H. Li, Y. Li, J. Liu, X. Wang and L. Wang, *J. Mater. Chem. A*, 2017, **5**, 25410.
- [12] J. Liu, Y. Zheng, D. Zhu, A. Vasileff, T. Ling and S. -Z. Qiao, *Nanoscale*, 2017, **9**, 16616.
- [13] C. Wang, B. Tian, M. Wu and J. Wang, *ACS Appl. Mater. Interfaces*, 2017, **9**, 7084.
- [14] Y. Yang, K. Zhang, H. Lin, X. Li, H. C. Chan, L. Yang and Q. Gao, *ACS Catal.*, 2017, **7**, 2357.
- [15] J. Zhang, T. Wang, D. Pohl, B. Rellinghaus, R. Dong, S. Liu, X. Zhuang and X. Feng, *Angew. Chem. Int. Ed.*, 2016, **55**, 6702.
- [16] J. Zhang, T. Wang, P. Liu, S. Liu, R. Dong, X. Zhuang, M. Chen and X. Feng, *Energy Environ. Sci.*, 2016, **9**, 2789.

- [17] Z. Xing, X. Yang, A. M. Asiri and X. Sun, *ACS Appl. Mater. Interfaces*, 2016, **8**, 14521.
- [18] A. Wu, C. Tian, H. Yan, Y. Jiao, Q. Yan, G. Yang and H. Fu, *Nanoscale*, 2016, **8**, 11052.
- [19] H. Zhu, J. Zhang, R. Yanzhang, M. Du, Q. Wang, G. Gao, J. Wu, G. Wu, M. Zhang, B. Liu, J. Yao and X. Zhang, *Adv. Mater.*, 2015, **27**, 4752.